Flame Kernel Drift in Homogeneous Isotropic Turbulence

T. D. Dunstan, K.W. Jenkins

School of Engineering, Cranfield University, Bedford MK43 0AL, UK

1 Introduction

Preliminary results from a study into the random drift of spherical flame kernels in freely decaying, homogeneous, isotropic turbulence, are presented. 3D DNS with single-step chemistry was used to investigate the displacement of kernels from their initial position due to the random perturbations of the small-scale (normally unresolved) eddies acting on the flame surface. A parallel series of cold-flow simulations was also carried out to assess the decaying characteristics of the various turbulent fields. The drift magnitude is found to vary depending on the particular level of reaction progress variable tracked, and a bias is shown to exist in the distribution of flame surface properties due to this differential drift effect.

In spark ignition engines the early stages of flame kernel development strongly depend on the movement of the kernel, due to heat transfer from the burned gasses to the electrodes [1]. Simulations of the combustion phase typically treat the early kernel, where it is small compared to the local turbulent length scales, as a coherent unit that is convected with the mean flow as a Lagrangian particle [2]. In the present work the additional component of drift due to turbulent fluctuations is studied in relation to the characteristics of the surrounding turbulence (integral length scale L_{11} and intensity u'). Global drift magnitude, the changing structure of the flame front and the distribution of flame surface across the kernel are examined.

2 Numerical Implementation

Simulations were carried out using the fully compressible DNS code SENGA. Non-dimensional transport equations for mass, momentum, and energy were solved in a cubic domain. A more complete description of the governing equations can be found in previous publications [3]. Navier-Stokes Characteristic Boundary Condition (NSCBC) outflows are used on all faces. Time stepping is carried out with a third-order Runge-Kutta scheme, and all spatial derivatives are calculated using tenth-order, explicit central-differencing.

The initial turbulent field was generated in Fourier space using the spectral method of Orszag [4], with a Schumann and Patterson energy spectrum (2.1) [5]. The magnitude of each Fourier mode is determined for a particular energy spectrum by specifying the peak wavenumber, K_p (which determines the integral length scale L_{11}), and turbulence intensity, u'. The phase angle is assigned using a pseudo-random number routine which allows multiple, unique realisations with similar turbulence properties. This method, in combination with the Schumann and Patterson spectrum, is known to give a good approximation of decaying turbulence in the final period, and allows control over its characteristics through variation of K_P and u' .

$$E(k) = 16\sqrt{\frac{2}{\pi}} u_{rms}^2 \frac{k^4}{k_p^5} e^{-2\left(\frac{k}{k_p}\right)^2} \tag{2.1}$$

Combustion is represented by a single-step, irreversible reaction where reactants $\rightarrow$ products, and a transport equation is solved for the reaction progress variable $c = (Y_p - Y_{p0})/(Y_{p\infty} - Y_{p0})$, where Y_p is the mass fraction of products, and varies from 0 in the fresh gasses to 1 in the fully burned. The reaction rate is determined by

Correspondence to : t.d.dunstan@cranfield.ac.uk

Arrhenius kinetics using a non-dimensional pre-exponential factor B^*, adjusted in each case to ensure a planar, unstretched laminar flame speed $S_L = 1$. Values for specific heat C_p, thermal conductivity λ, diffusivity ρD, and dynamic viscosity μ are assumed constant, and a unity Lewis number $Le = \lambda/\rho C_p D$ is used in all cases.

3 Results

A list of parameters used for each case is given in Table (3.1). Cold-flow results were obtained using the same initial turbulence parameters as those shown below. Reaction rate constants and thermo-diffusive properties are the same in all cases and are representative of a stoichiometric methane-air flame at atmospheric pressure.

Case	K_p (x2π)	u'	Common parameters	
I	2	4	Le =1	$\gamma = 1.4$
II	4	4	Pr = 0.7	Grid points (164^3)
III	6	4	Sc = 0.7	Domain size L = 1.7 ($\approx 1.6\delta_{th}$)
IV	2	6	$\tau = 3.0$	Laminar flame speed $S_L = 1.0$
V	4	6	$\beta = 6.0$	Density ratio $\rho_0/\rho_b = 4$
VI	6	6		

Table 3.1 Database parameters

To obtain information on the ensemble-average behaviour of the flames, six repetitions are carried out for each case using independent, randomly generated initial fields for all simulations in the database. Since this sample size is relatively small, a statistical analysis of the cold-flow turbulence properties is first presented to demonstrate the degree of uncertainty present.

A distinction between the terms 'mean' and 'ensemble-average' should be noted: 'mean' here refers to the domain-average value for any specific simulation, such as the mean isosurface radius c=c* which is the mean of all local radii values from a single flame kernel. 'Average' or 'ensemble-average' is used to refer to the sample-mean of all replicates in a particular case. In general, ensemble-average values are used unless otherwise stated.

To initialise the flame, velocity and progress variable fields from a precomputed steady, spherical, laminar flame solution are superimposed onto the turbulence. The initial kernel has a radius $r_0 \approx 1.7\delta_{th}$, where r_0 represents the region of fully burned gas. δ_{th} is the laminar, unstretched flame thermal thickness, defined as $\delta_{th}=(T_{ad}-T_0)/\max|(\partial T/\partial n)|$, where T_{ad} is the adiabatic flame temperature, T_0 is the temperature in the fresh gasses and n is the distance in the flame surface normal direction..
The kernel centre position (Eq. 3.1) is taken as the mean value of N sample positions on a given c* isosurface for each coordinate direction i.

$$\overline{x_{ci}} = \left(\sum x_i / N\right)\Big|_{c=c^*} \tag{3.1}$$

Kernel drift s_c, is defined as the absolute displacement of a specific isosurface centre from its initial position x_0: $s_c = \sqrt{\left(x_{ci} - x_0\right)^2}$. If a distinction between different isosurfaces is not necessary the c*=0.8 isosurface (representative of the reaction layer) is used.

Mean and variance of the local radii are also collected to provide information on the growth and wrinkling of the flame front. Isosurface centre and radius statistics were evaluated for 10 different c* values, where c* = 0.1, 0.2,...,1.0, and data were collected until the outer edge of the flame (c = 0.1 isosurface) reached the boundary.

3.1 Turbulence decay properties

To characterise the turbulence/flame interaction, two non-dimensional numbers are considered, following Peters [6]: The Damkohler number $Da = L_{11}/u't_f$, which relates the flame time to the energy-containing range, and the Karlovitz number $Ka_r = t_{fr}/t_\eta$, where $t_\eta = \eta/u_\eta$, which represents the ratio of the flame time to the Kolmogorov time scale. The Karlovitz number used here refers to the inner reaction layer of the flame (estimated as $0.1\delta_{th}$).

For Da >>1 and Ka_r << 1, the assumption is that there is sufficient separation of scales between the turbulence and flame to allow the flame structure to remain quasi-laminar. Estimated values of Da and Ka_r for this database were ≈ 1 and ≈ 0.4 respectively, suggesting that this assumption may not be valid, however, inspection of the flame kernel profiles show that, due to the more rapid decay of u' (Fig 3.1.1(c)) for the high peak wavenumbers, all flames in the database remain in the thickened-wrinkled or thin-reaction-zones regimes while drift statistics are being collected.

Initial integral length scales, L_{11}/δ_{th}, calculated from the cold-flow simulations, produce values ranging from 2.4 – 3.3 (average 3.1) for K_p = 2, 1.5 – 1.8 (average 1.7) for K_p = 4, and 1.0 – 1.2 (average 1.1) for K_p = 6, and this variation is reflected in the turbulent Reynolds numbers ($Re_t = u'L_{11}/\nu$). Fig 3.1 (a and b) show time-dependent values of Re_t taken from the cold-flow results.

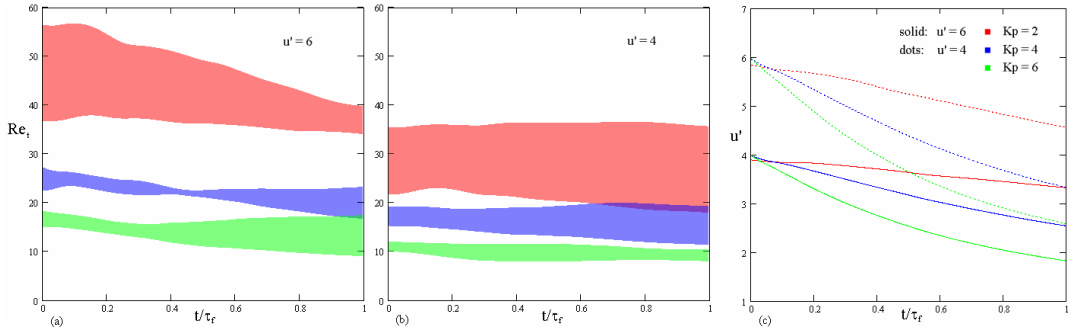

Fig 3.1 Turbulence Reynolds number (a and b): 95% confidence intervals shown assuming a t-distribution with 5 DoF; and (c) turbulence intensity u'/S_L.

3.2 Kernel Structure and drift

An increase in the ensemble-averaged mean flame thickness, $\langle \bar{r}_{c=0.1} - \bar{r}_{c=1} \rangle$, over the initial laminar value of 20%-30% can be observed for all cases after t = $0.5t_f$. Significant increases in the turbulent flame speed, $S_t = (\rho_b/\rho_0)\, d(\bar{r}_{c=0.8})/dt$, over the laminar flame speed are only observed for the lowest peak wavenumber, K_p = 2, due in part to the more rapid decay of kinetic energy at the higher peak wavenumbers. Comparison of the variance of the local radii, which gives an indication of the wrinkling of each isosurface, shows a clear positive correlation with the turbulent Reynolds number.

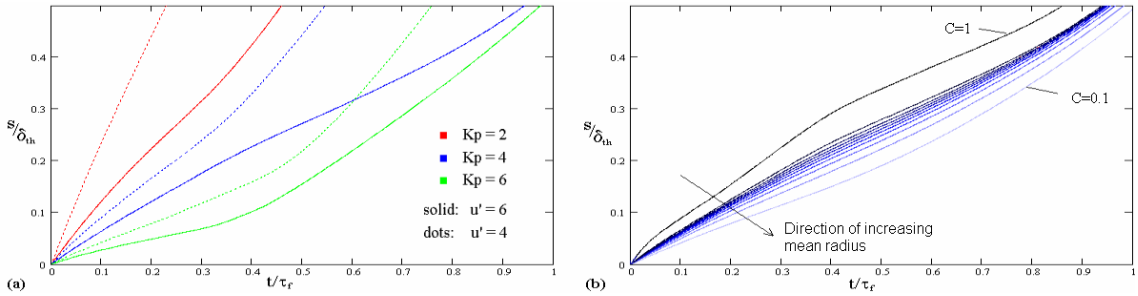

Fig 3.3 (a) Global displacement (c=0.8 isosurface). (b) Average displacement of all isosurfaces for case II

The global kernel displacement, s, for c=0.8 isosurfaces (Fig 3.2.3(a)) shows that K_p, u' and their interaction, all have a significant effect on the global drift, and this suggests that differences in the kernel growth rate (and S_t) have only a negligible effect on the drift magnitude over these time scales.

An important trend is found in the difference in drift magnitude experienced by different isosurfaces, as illustrated in Fig 3.2.3(b): In all cases, drift is greater for isosurfaces with smaller mean radii. This differential drift effect is present at all times during the simulations, and is found consistently in individual simulations as well as at the ensemble average level.
The direction of drift for each isosurface within a particular simulation is approximately the same at any point in time, and this, combined with the differential drift effect, implies that an uneven distribution of progress variable gradients should be found throughout the flame brush. More specifically, the gradient magnitude ($\sigma = |\nabla c|$) should show a positive correlation with its position along a vector aligned with the instantaneous direction of kernel drift.
Confirmation of this using the present database presents some difficulties since the effect was not anticipated, however, initial results (Table 3.2) suggest that the prediction is correct and that further investigation is warranted.
For any position in the domain $\vec{x}$, its projection p_c on the instantaneous drift direction unit vector is $p_c = x_i \hat{s}_{ci}$, where $\hat{s}_{ci} = s_{ci}/|s_c|$. Here, σ is not conditioned on a c^* isosurface – all values in the domain are considered.

Case	I	II	III	IV	V	VI
K_P	2	4	6	2	4	6
u'	4			6		
Correlation (p_c , σ)	**0.127**	**0.075**	**0.054**	**0.150**	**0.111**	**0.064**

Table 3.2 Correlation of σ and projection p_c along instantaneous direction of drift for the c=0.8 isosurface.

As the values in Table 3.2 show, the correlations are weak. However, the number of data used in the calculation was large ($\approx 10^6$) and the probability of error is therefore low. Also significant is the fact that the relative magnitude of the correlation corresponds qualitatively to the mean turbulent Reynolds number for each case, suggesting that the effect is a predictable function of the turbulence properties.
Confirmation of this phenomenon will be the subject of future work where the limitations of the present database can be fully addressed.

Acknowledgements

This work was supported by the Engineering and Physical Sciences Research Council, UK (EPSRC), and Cranfield University High Performance Computing Facility.

References

[1] Heywood, J. B. (1994), "Combustion and its Modelling in Spark Ignition Engines", *COMODIA 94,* 1994

[2] Duclos, J. M. and Colin, O. (2001), "Arc and Kernel Tracking Ignition Model for 3D Spark-Ignition engine calculations", *5th International Symposium on Diagnostics and Modelling of Combustion in Internal Combustion Engines,* 2001, pp. 343.

[3] Jenkins, K. W. and Cant, R. S. (1999), "Direct Numerical Simulation of Turbulent Flame Kernels", *Proceedings of the 2nd AFSOR conference on LES and DNS,* 1999, Rutgers, Kluwer, pp. 192.

[4] Orszag, S. A. (1969), "Numerical methods for the simulation of turbulence", *The Physics of Fluids Supplement II, American Institute of Physics,* vol. 12, pp. 250-257.

[5] Schumann, U. and Patterson, G. S. (1978), "Numerical study of pressure and velocity fluctuations in nearly isotropic turbulence", *Journal of Fluid Mechanics,* vol. 88, no. 4, pp. 685-709.

[6] Peters, N. (2000), Turbulent Combustion, Cambridge University Press, Cambridge, UK.